$E0$ decay of the first excited 0^+ states in ^{26}Mg and ^{30}Si

J. C. Adloff, K. H. Souw, D. Disdier, F. Scheibling, and P. Chevallier
Centre de Recherches Nucléaires, Université Louis Pasteur, Strasbourg, France

Y. Wolfson
The Weizmann Institute of Science, Rehovot, Israël

(Received 29 July 1974)

A new method was used to measure $E0$ π-decay branching ratios. A plastic scintillator pair spectrometer of high efficiency (3%) was used. It consists of four detectors. Two of them, very thin, select the electrons; the other two, thick, help to measure their energies. An annular counter ($\Omega = 0.10$ sr), working in coincidence with the spectrometer, allows the selection of the π decay relevant to the 0^+ excited state and the determination of its population yield. The reactions ^{23}Na$(\alpha, p)^{26}$Mg(3.58 MeV)(π) and ^{27}Al$(\alpha, p)^{30}$Si(3.79 MeV)(π) have been used to study the $E0$ π decay of the first excited 0^+ state in ^{26}Mg and ^{30}Si. Pair spectra from the spectrometer were recorded in coincidence with protons in two-dimensional arrays. From the coincidence spectra the values for Γ_π/Γ are found to be $(5.1 \pm 0.7) \times 10^{-3}$ and $(2.6 \pm 0.6) \times 10^{-3}$, respectively, for ^{26}Mg(3.58 MeV) and ^{30}Si(3.79 MeV). When combined with the available lifetimes of these states, these ratios yield $\langle M \rangle_\pi = (3.0 \pm 0.25)$ fm^2 (^{26}Mg) and (1.4 ± 0.2) fm^2 (^{30}Si) for the monopole matrix elements.

[NUCLEAR REACTIONS ^{23}Na(α, p), $E = 6.44$ MeV; ^{27}Al(α, p), $E = 3.88$ MeV; ^{26}Mg, ^{30}Si measured $E0$ branching ratio. Deduced $E0$ matrix elements. Natural targets.]

I. INTRODUCTION

There is no doubt that in even-even nuclei $E0$ matrix element measurements are important tools in the study of nuclear structure. The $E0$ matrix element relevant to transitions from the first excited 0^+ state to the ground state are related to the overlap of the wave functions of the two states and to the mean configuration radii. Moreover, if in the excited state one proton changes its principal quantum number, the monopole operator $\sum_p r_p^2$ directly connects this type of configuration to the main configuration in the other state. The most extensive theoretical work has been done on the $E0$ decay in doubly magic nuclei like ^{16}O and ^{40}Ca, and in ^{12}C in which the properties of the first excited 0^+ state play an important astrophysical role.[1]

In even-even nuclei very few $E0$ transitions have actually been studied. Below $A \approx 90$, three principal methods were used to measure $E0$, $0^+ \rightarrow 0^+$, transitions:

(1) In some cases the monopole internal pair emission width can be measured in (e, e') experiments as in ^{16}O (Ref. 2), ^{12}C (Refs. 3–6), and ^{4}He (Ref. 7).

(2) Lifetime measurement methods have been used for the first excited state where $E0$ decay occurs predominantly in ^{16}O (Ref. 8), ^{40}Ca (Refs. 9, 10), ^{72}Ge (Ref. 11), and ^{90}Zr (Refs. 9, 12, and 13).

(3) A powerful method was developed by the Brookhaven group for cases where the $E0$ decay to the ground state is strongly unfavored by the presence of a γ decay.[14] The use of an intermediate image magnetic spectrometer in their work has allowed measurement of $E0$ branching ratios and matrix elements in ^{10}Be (Ref. 15), ^{12}C (Ref. 16), ^{14}C (Ref. 17), ^{58}Ni (Ref. 18), ^{54}Fe (Ref. 19), and ^{70}Ge (Ref. 13). This technique was also used in ^{18}O (Ref. 20). Sometimes $E0$ branching ratios can be obtained by other methods as in ^{48}Ca (Ref. 21), ^{42}Ca (Refs. 22 and 23), and ^{36}S (Ref. 24).

Except for ^{16}O, ^{40}Ca, ^{72}Ge, and ^{90}Zr, $E0$ transitions from the first excited 0^+ to the ground state are usually in competition with an $E2$ γ cascade via a $J^\pi = 2^+$ intermediate state which represents almost the total width of the excited 0^+ state. From the preceding articles an order of magnitude of Γ_π/Γ can be estimated to be $\approx 10^{-3}$ however, with some exceptions.[18,24] One should notice that in the $1p$ and $2s$-$1d$ shells, the branching ratio for $E0$ conversion electron emission is usually far smaller than the $E0$ pair branching ratio.[25] For example in ^{40}Ca, $\Gamma_{ce}/\Gamma_\pi = (6.94 \pm 0.20) \times 10^{-3}$.[26] The alternative process of two photon emission is also negligibly small.

In view of the small $E0$ branch one has to detect $e^\pm$ pairs efficiently. Furthermore, the detection of γ rays from the strong γ cascade can interfere with the detection of the pairs. Also in the usual

presence of higher multipolarity pair production from many levels, a high resolution (or some other method) must be employed to identify the pairs originating from a given level. Some of these problems have been solved by the use of the intermediate image spectrometer which has allowed the measurement of many $E0$ branching ratios for $A < 90$ nuclei.

In this work we employ a new experimental method to measure $E0$ branching ratios. The method is related to that of Devons[8, 27-29] which has been used extensively in Strasbourg.[30-33] We use two high efficiency double coincidence plastic scintillator telescopes for pair detection. A reduced sensitivity to γ-γ detection was obtained by using thin plastic scintillators to detect the electrons. The rather poor energy resolution of the plastic scintillators was compensated by detecting the pairs in coincidence with the particles feeding the 0^+ excited level through (particle, particle) nuclear reactions. From bidimensional spectra a true identification of the pairs was possible together with a normalization to the singles heavy-particle spectra.

As will be explained in Sec. II, our measurements give directly the ratio Γ_π/Γ. The partial $E0$ lifetime and the corresponding $E0$ matrix element can be deduced from these ratios with the knowledge of the 0^+ level lifetime which is available from other measurements. In this paper we present the results of $E0$ branching ratios measurements relevant to the first excited 0^+ states in ^{26}Mg and ^{30}Si formed in (α, p) nuclear reactions.

II. EXPERIMENTAL METHOD

A. Apparatus

Figure 1 shows a schematic diagram of the experimental arrangement. A small target chamber was employed so as to have large solid angles for the pair detection. These solid angles are defined by the geometry of the thin plastic scintillators. These were obtained by bending 0.2-mm-thick NE102 foils at 100°C in an oven. The resulting half cylindrical detectors (2.9-cm-long with a curvature radius of 9 mm) were connected by an optical cement onto light pipes. The light pipes are seen by low-noise 56DVP photomultipliers.

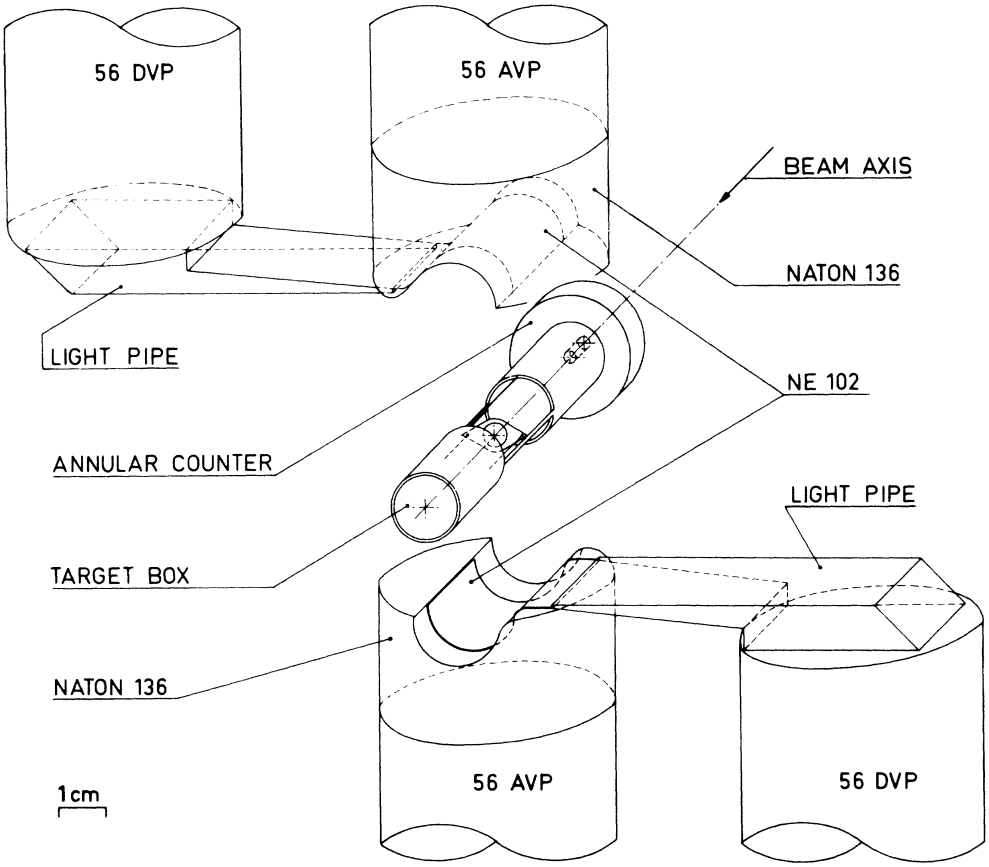

FIG. 1. Schematic diagram of the experimental setup. The plastic scintillator telescopes are represented away from the target chamber.

Another similar set of thin detectors and light pipes was used; it was obtained from 0.4-mm-thick NE102A foils. The full energy plastic detectors are 2.54-cm-thick×5.08-cm-diam Naton 136 scintillators coupled to 56AVP photomultipliers. A half cylindrical hollow allows them to receive the thin detectors. Each telescope is in a separate housing (not represented in Fig. 1) which is made light tight in front of the thin detectors by a 0.02-mm-thick aluminum foil. Light tightness between the thin and thick detectors is ensured by an aluminized Mylar foil. The two telescopes fit around the target chamber. This chamber is a 17-mm-diam–1-mm-thick stainless steel tube which is tailored so as to present four 3-cm-long openings in front of the telescopes. These openings are rendered vacuum tight by a 0.08-mm-thick copper foil (not represented in Fig. 1). The target is placed in the middle of the chamber perpendicular to the beam axis. One telescope subtends the angular ranges: $\theta = 31°–149°$, $\phi = 7°–86.5°$, $93.5°–173°$, around the beam spot, where the notations θ and ϕ have the usual meaning.

The quadrupole coincidences in the telescopes are put into coincidence with pulses from a 180° annular counter. This detector, the inclusion of which makes for the originality of the system, detects the particles which fed the excited 0^+ state through an appropriate nuclear reaction. In the measurements described here it was a 300-μm-thick, 150 mm^2 silicon surface barrier detector located 3.8 cm from the target. This detector is collimated with a circular aperture 6.3 mm in diameter located at 16 mm from the target.

Figure 2 shows the block diagram of the associated electronics. All photomultiplier outputs are anode pulses. This allows the use of fast linear gates in the proportional chains of the full energy plastic detectors in order to avoid pulse pileup at high counting rates. A 30 nsec gate opening time was chosen. The busy signal from the linear stretchers was 4 μsec wide. The time resolution of the fast coincidence circuits typically was chosen to be 15 nsec. The quadrupole coincidence pulses from the telescopes started a time-to-amplitude converter (TAC) for which the stop pulses were taken from the annular detector. A 20 nsec time window was chosen for

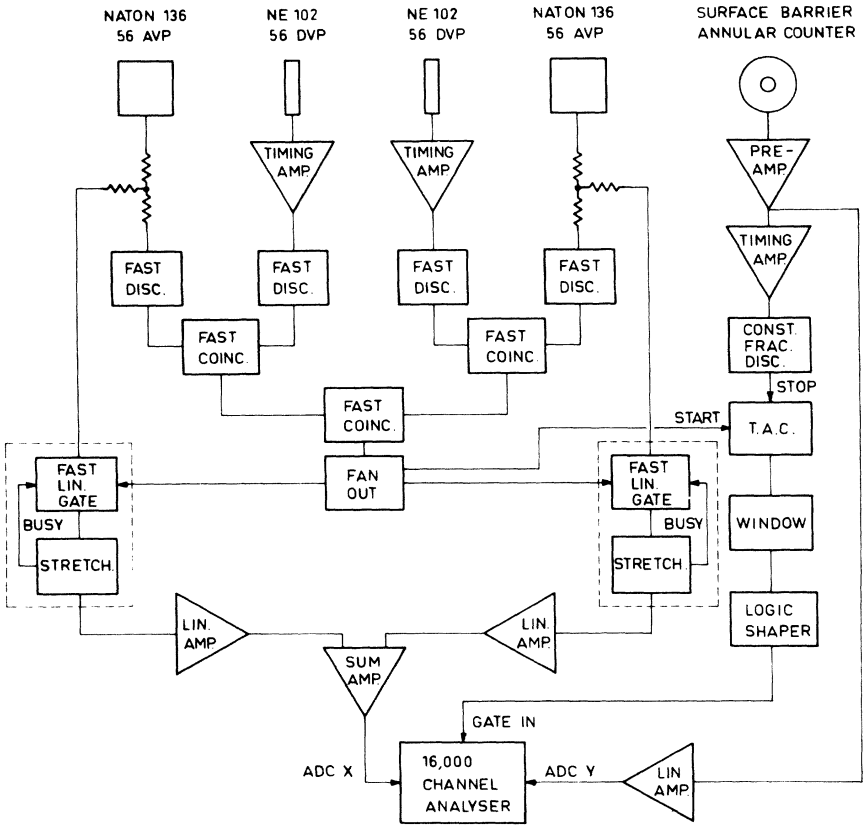

FIG. 2. Block diagram of the electronics. All photomultiplier outputs are anode pulses. The fast linear gate open time is 30 nsec. The busy signals from the linear stretcher are 4 μsec wide.

the TAC . The fivefold coincidence pulses were used to open the gate of an Intertechnique 16000-channel analyzer. This analyzer operating in a two-dimensional mode was used to store the summed energy spectrum of the pairs as a function of particle energy. At the same time the sampled singles spectrum from the annular detector was stored in the $X=0$ channels.[34]

B. Telescope efficiency measurements

The experimental arrangement just described directly allows measurements of the ratio of the partial $E0$ width to the total width of the 0^+ level under study. This ratio is given by:

$$\frac{\Gamma_\pi}{\Gamma} = \frac{N_{\pi p}/(\epsilon\Omega)_\pi}{N_p} . \quad (1)$$

The ratio $N_{\pi p}/(\epsilon\Omega)_\pi$ is the number of pair-particle coincidences divided by the total absolute pair efficiency of the telescopes. N_p is the singles yield of the heavy particles feeding the 0^+ excited level. If one deals with $E0$ transition energies around 3.5 MeV which is usually the case in the $2s$-$1d$ shell, it is convenient to use the almost 100% monopole decay of the 3.35 MeV level in ^{40}Ca to measure the pair efficiency of the telescopes.

The ^{40}Ca(p, p_1) resonance at $E_p = 5.41$ MeV was used to populate the ^{40}Ca(3.35 MeV, 0^+) level. A proton beam of typically 50 nA was delivered by the 5.5 MV Van de Graaff onto a beam spot whose diameter was about 1 mm. Natural calcium targets, 80-μg/cm^2-thick, were made by evaporation onto 40-μg/cm^2-thick carbon backings. A typical pair spectrum of the 3.35 MeV monopole decay is shown in Fig. 3. It results from the projection in the p_1 region of the corresponding pair energy vs proton energy spectrum (not represented). The fast discrimination on the electron spectra was set at 400 keV in order to avoid pulses from the 511 keV γ-ray Compton interactions. This threshold was also chosen in the ^{26}Mg and ^{30}Si measurements. The factor $(\epsilon\Omega)_\pi$ is given by the ratio $N_{\pi p}/N_p$ where $N_{\pi p}$ is taken from a spectrum such as shown in Fig. 3 and N_p from the corresponding singles proton spectrum.

With the discrimination set at 400 keV, typical pair efficiencies are 3% in the case of the telescopes mounted with 0.2-mm-thick ΔE detectors and 6% for the 0.4-mm-thick ones. The efficiency loss in the first case is due to the 61% electron (positron) efficiency of the ΔE detectors resulting from poor light transmission to the 56DVP photomultipliers. Although the use of the thinner plastics leads to an efficiency loss, it allows measurements of lower energy $E0$ transitions than do the 0.4-mm-thick ones, for which the counting efficiency was nearly 100%.

For transition energies higher than the 3.35 MeV ^{40}Ca $E0$ decay, such as those in ^{26}Mg and ^{30}Si, the pair efficiency measured in the ^{40}Ca case has to be corrected slightly in order to take into account the broader electron (positron) spectrum. These corrections were approached by calculating the pair efficiencies, for different transition energies, as a function of the total energy discrimination on the $e^\pm$ spectra introduced by the copper, aluminum, and NE102 (NE102A) absorbers (see Sec. II A) and the electronic discrimination considered as a variable parameter. The computation takes into account the theoretical shape of the $e^\pm$ monopole spectra, the detection geometry and the experimental energy resolution and straggling from the absorbers. These later were obtained for the whole range of $e^\pm$ energies by interpolating and extrapolating from spectral shapes measured for monoenergetic electrons from ^{137}Cs and ^{207}Bi sources. The β particle attenuation curves for the absorbers were assumed to be the same as those for aluminum,[35] when the curves are expressed in mg/cm^2. This assumption was found to be true to within 10% in the case of the source measurements. The results of the calculations are shown in Fig. 4 by the solid lines for transition energies of 3.35, 3.58, and 3.93 MeV. In the figure the efficiencies are reported in function of $E_t/(K/2)$, where E_t is the energy threshold on the $e^\pm$ spectra. The ratio

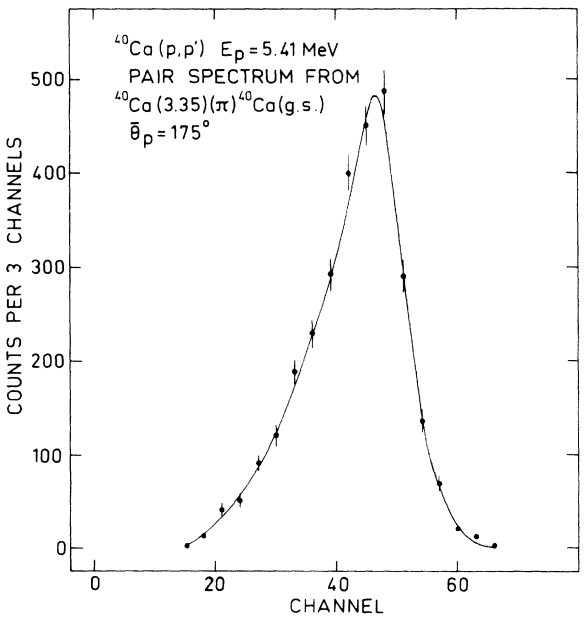

FIG. 3. Pair spectrum from the decay of the ^{40}Ca(3.35 MeV, 0^+) state in coincidence with the protons from the ^{40}Ca$(p, p_1)^{40}$Ca reaction.

$K/2$ is half the kinetic energy of the pairs. Also given in the figure are measured efficiencies for the 3.35 MeV decay of ^{40}Ca for different discriminator settings. E_t is evaluated as stated above. The experimental energy discriminator settings ranged from 200 to 700 keV. In the region $0.48 < E_t/(K/2) < 0.61$ where efficiency corrections were made in the ^{26}Mg and ^{30}Si cases, the agreement between the calculated ^{40}Ca efficiencies and the measured ones are good. Therefore we used the calculated efficiency curves for 3.58 and 3.79 MeV (^{26}Mg, ^{30}Si) to get the absolute efficiencies corresponding to a discriminator setting of 400 keV.

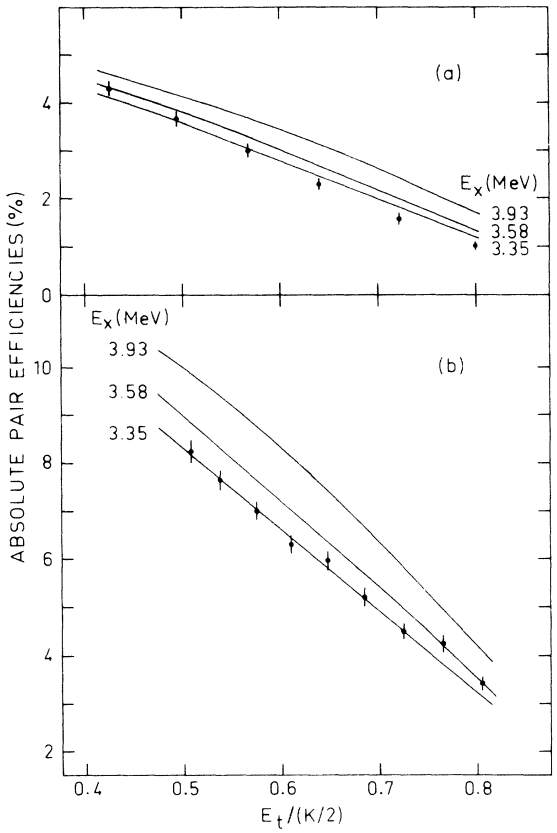

FIG. 4. Absolute pair efficiencies of the plastic scintillator telescopes in function of $E_t/(K/2)$. The meaning of E_t is the total energy discrimination on the $e^{\pm}$ spectra (see Sec. II B) and $K/2$ is half the kinetic energy of the pair. The curves are calculated for transition energies $E_x = 3.35$, 3.58, and 3.93 MeV. The experimental points are relevant to the 3.35 MeV monopole transition of ^{40}Ca (see Sec. II B). (a) Results for the telescopes with 0.2-mm-thick NE102 ΔE counters. The electronical energy discriminations range from 200 to 700 keV in 100 keV steps. (b) Results for the telescopes with 0.4-mm-thick NE102A ΔE counters. The discriminations range from 250 to 650 keV in 50 keV steps.

C. ^{26}Mg(3.58 MeV, 0^+)(π)^{26}Mg(g.s.) decay

A checking procedure consisting of a pair efficiency measurement using the ^{40}Ca(p, p') reaction (see Sec. II B) was made before each run under the same experimental conditions used for other nuclei.

The reaction ^{23}Na(α, p)^{26}Mg was used to populate the first excited 0^+ state in ^{26}Mg at $E_x = 3.58$ MeV.

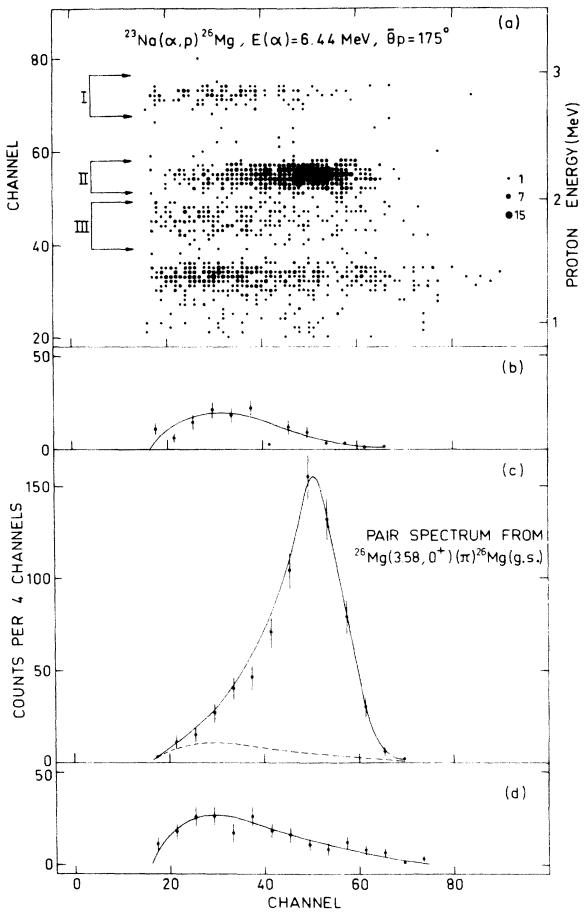

FIG. 5. (a) Partial proton energy vs pair energy spectrum from ^{23}Na(α, p)^{26}Mg(π, γ) and ^{19}F(α, p)^{22}Ne(γ) at $E_\alpha = 6.44$ MeV, $\bar{\theta}_p = 175°$. The pair decay of the ^{26}Mg(3.35 MeV, 0^+) state is in region II. Events in regions I and III are γ-γ interactions in the telescopes in coincidence with protons feeding, respectively, the 2.94 MeV state in ^{26}Mg and the 3.94 MeV state in ^{26}Mg plus the 3.36 MeV state in ^{22}Ne. The number of counts is indicated by size of dots. The projection of the spectrum in (a) onto the proton energy axis is represented in Fig. 6. The projections of regions I, II, and III onto the pair energy axis are represented, respectively, in part (b), (c), and (d) of this figure. The dashed line in part (c) is the calculated γ-γ contribution from the 3.58 MeV → 1.81 MeV → g.s. γ-ray cascade assuming the shape in part (d), the solid line is taken from Fig. 3.

A $^4He^{++}$ beam of typically 0.2 μA was used to bombard 300 $\mu g/cm^2$ NaF targets that had been evaporated onto 250 $\mu g/cm^2$ gold backings. A resonance in the $^{23}Na(\alpha, p_3)^{26}Mg(3.58\ MeV)$ reaction situated at $E_\alpha = 6.44$ MeV was chosen. The annular counter was covered by a 30-μm-thick aluminum absorber which ensured that only protons were detected.

Figure 5(a) shows a part of the two-dimensional pair energy vs proton energy spectrum, the result of a 9 h measurement. The projection onto the proton energy axis of this spectrum is represented in Fig. 6(b) together with the associated direct 1/32 sampled singles proton spectrum [Fig. 6(a)]. The ground state pair decay of the 3.58 MeV level in ^{26}Mg is clearly in evidence in region II of Fig. 5(a) which is projected onto the pair energy axis in Fig. 5(c). The spectral shape represented in Fig. 3 is used in fitting the solid curve in Fig. 5(c). The dashed curve represents the calculated γ-γ contribution from the 3.58 $(0^+) \rightarrow$ 1.81 MeV $(2^+) \rightarrow$ g.s. γ cascade. The shape of the curve is taken from the measured γ-γ spectral shape resulting from the 100% 3.36 MeV $(4^+) \rightarrow$ 1.27 MeV $(2^+) \rightarrow$ g.s. cascade in ^{22}Ne and from the cascades coming from the 3.94 MeV level in ^{26}Mg [62% to the 2.94 MeV (2^+) state, 38% to the 1.81 MeV (2^+) state].[36] All these decays are in region III of Fig. 5(a). The corresponding projection onto the pair energy axis is represented in Fig. 5(d). The yield of the γ-γ interaction per detected proton is obtained by the mean value of the yield in region III, the 90% 2.94 MeV $(2^+) \rightarrow$ 1.81 MeV $(2^+) \rightarrow$ g.s. cascade[36] in ^{26}Mg [region I of Fig. 5(a)] and the 100% 3.81 MeV $(3^-) \rightarrow$ 2.17 MeV $(2^+) \rightarrow$ g.s. cascade[36] in ^{38}Ar (not represented). In all these cases cross-over pair emission of high multipolarities is negligibly small in view of the low intensity of the ground state γ transition.[36] A mean value of $(1.5 \pm 0.3) \times 10^{-5}$ γ-γ interactions per detected proton was found for the telescopes with 0.2-mm-thick ΔE scintillators and $(2.3 \pm 0.5) \times 10^{-5}$, when 0.4-

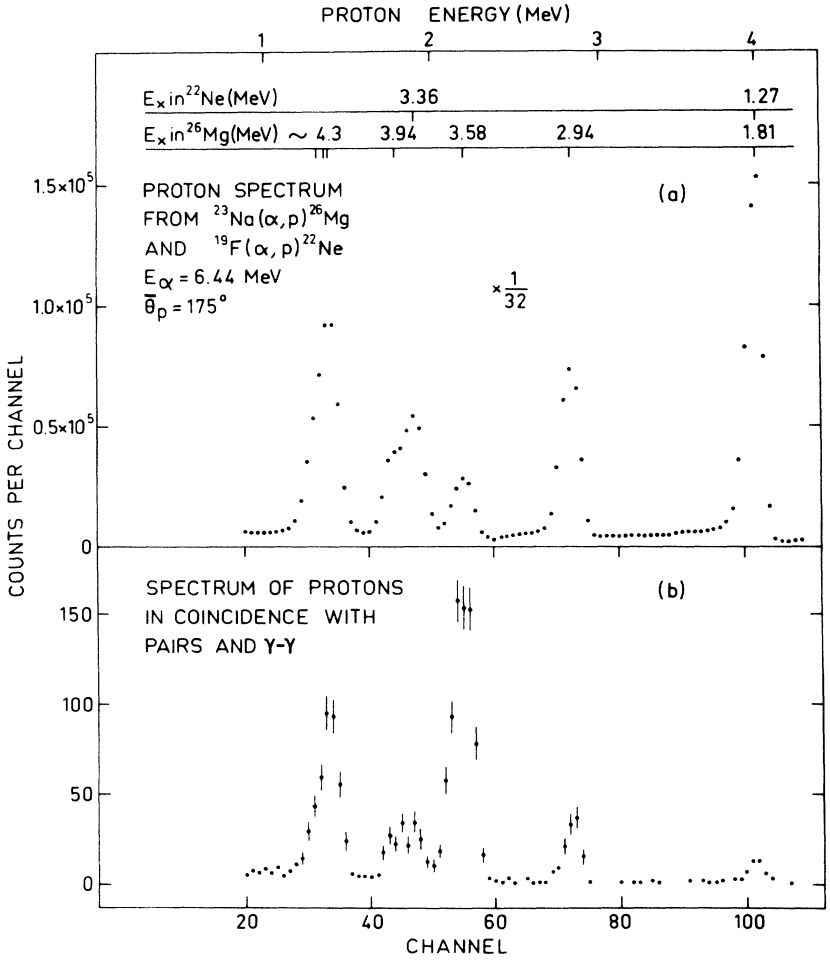

FIG. 6. (a) 1/32 sampled direct proton spectrum taken simultaneously with the spectrum of Fig. 5(a). (b) Projection onto the proton energy axis of the two-dimensional spectrum a part of which is shown in Fig. 5(a).

mm-thick ΔE counters are used.

By using relation (1), where $N_{\pi p}$ is taken from the spectrum Fig. 5(c), N_p is obtained from the yield of the peak at channel 55 of Fig. 6(a) and $(\epsilon\Omega)_\pi$ is calculated to be $(3.9 \pm 0.5)\%$ (see Sec. II B), the branching ratio of the monopole decay of the 3.58 MeV state in ^{26}Mg is found to be $\Gamma_\pi/\Gamma = (4.9 \pm 0.6) \times 10^{-3}$. A similar measurement done with the telescopes mounted with the 0.4-mm-thick ΔE counters with $(\epsilon\Omega)_\pi = (7.3 \pm 0.8)\%$ yields $\Gamma_\pi/\Gamma = (5.3 \pm 0.7) \times 10^{-3}$. We take $\Gamma_\pi/\Gamma = (5.1 \pm 0.7) \times 10^{-3}$, the mean value of the two measurements, as our final result. Recent measurements of the lifetime of the 3.58 MeV state of (9.5 ± 0.7) psec[37] and (9.6 ± 1.2) psec[38] have been given. When combined with the mean weighted value of these measurements the value of our branching ratio yields $\tau_\pi = (1.87 \pm 0.28)$ nsec for the partial mean lifetime of $E0$ decay to the ground state. The value of the matrix element is calculated from the value of τ_π by using formulas, tables, and graphs given by Wilkinson in his review article on $E0$ pair transitions.[39] The value for the monopole matrix element in ^{26}Mg is $\langle M \rangle_\pi = (3.0 \pm 0.25)$ fm^2.

D. ^{30}Si(3.79 MeV, 0^+)(π)^{30}Si(g.s.) decay

The experimental procedure followed in the ^{30}Si measurements was the same as in the ^{26}Mg case. The ^{27}Al$(\alpha, p)^{30}$Si reaction was used to populate the 3.79 MeV first excited 0^+ state in ^{30}Si. A ^{4}He$^+$ beam of 0.2 μA was used to bombard 160 μg/cm^2 self-supporting aluminum targets. The annular detector was covered by a 20-μm-thick aluminum absorber. A resonance at $E_\alpha = 3.38$ MeV which excites both the 3.79 MeV (0^+) and 3.77 MeV (1^+) states in ^{30}Si was chosen. However, in the spectra from the annular detector the proton groups feeding the two states could not be separated. It was therefore necessary to use a different experimental configuration to obtain the singles yield. The latter could be obtained by detecting with a good resolution the γ rays originating from the decays of the 0^+ and 1^+ levels in coincidence with the corresponding unresolved protons group. In order to avoid corrections due to the proton angular distribution, the same solid angle for the annular counter as in the $\pi - p$ measurement was adopted. The γ-ray cascades from the 1^+ level [$42 \pm 5\%$ to the g.s., $58 \pm 5\%$ to the 2.23 MeV (2^+) state][40] and from the 0^+ (100% to the 2.23 MeV state)[40] level were detected with a 80 cm^3 Ge-Li detector. The detector was placed at 55° to the beam axis with the surface of the germanium crystal 2 cm from the target. The axial symmetry for the proton detector and spins 0 and 1 of the 3.79 and 3.77 MeV states ensured that the p_4-γ [3.79 MeV → 2.23 MeV (2^+)] correlation is isotropic and that the p_3-γ (3.77 MeV → 2.23 MeV) correlation is limited to the $P_2(\cos\theta)$ term. Thus by detecting the γ rays at a zero of the $P_2(\cos\theta)$ Legendre polynomial, the necessity of doing a detailed angular correlation measurement for the 1^+ state is avoided.

Figure 7 shows a part of the coincident γ-ray spectrum of the 3.77 MeV (1^+) → 2.23 MeV (2^+) and 3.79 MeV (0^+) → 2.23 MeV (2^+) decays. This spectrum results from the projection in the p_3, p_4 region of the corresponding bidimensional γ-ray energy vs proton energy spectrum (not represented) in which the zero channel of the γ-ray energy axis was appropriately shifted. From the spectrum of Fig. 6 and from the known $(58 \pm 5)\%$ branching ratio of the 1^+ state via the 2.23 MeV state we deduce the value $N_{p_4}/(N_{p_3} + N_{p_4}) = 0.37 \pm 0.03$. The symbols N_{p_3} and N_{p_4} are, respectively, the unresolved singles proton yields as detected in the annular detector for the 3.77 MeV (1^+) and 3.79 MeV (0^+) states.

Figures 8 and 9 show the result of a 15 h run with the pair spectrometer. The proton spectra represented in Fig. 8 have the same meaning as in the ^{26}Mg case (see Sec. C). The pair spectrum of Fig. 8 is obtained by projecting the events between proton channels 11–20 (see Fig. 8) of the pair energy vs proton energy spectrum (not represented). The calculated γ contribution in the spectrum of Fig. 9 (dashed line) is the correction for the γ-ray decays of the 0^+ and 1^+ levels. More-

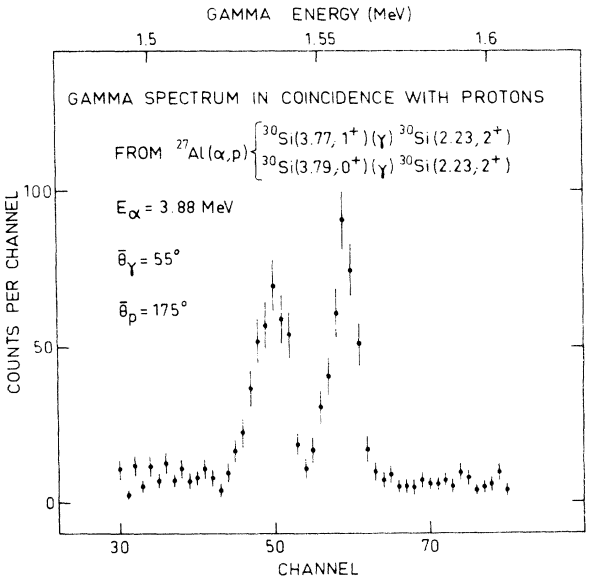

FIG. 7. Partial γ-ray spectrum in coincidence with the protons of ^{27}Al$(\alpha, p)^{30}$Si(3.77 MeV and 3.79 MeV). The broadening of the peak at channel 50 from the 3.77 MeV → 2.23 MeV transition is due to Doppler effect.

over the 42% γ-ray ground state transition from the 1^+ level allows for a small $M1$ internal pair emission yield in the spectrum of Fig. 9. This yield was evaluated by measuring the ^{38}Ar[3.94 MeV $(2^+) \rightarrow$ g.s.] $E2$ internal pair emission in competition with the 93.8% γ-ray ground state decay[40] in the pair spectrometer. For the $E2$ pair decay we found $N_{\pi p}(E2)/N_p = (5.0 \pm 1.0) \times 10^{-5}$ detected coincident pairs per detected proton. A similar measurement for the ^{18}O[3.92 MeV $(2^+) \rightarrow$ g.s.] $E2$ pair decay gave $N_{\pi p}(E2)/(N_p \times 0.15) = (6.8 \pm 3.0) \times 10^{-5}$ where 0.15 is the 15% γ-ray branching ratio of the 3.92 MeV state to the ground state.[41] The $M1$ pair contribution from the ^{30}Si(3.77 MeV) state in the spectrum of Fig. 9 was calculated by using $N_{\pi p}(E2)/N_p = (5.0 \pm 1.0) \times 10^{-5}$, the correction for $E2$ to $M1$ internal pair production[42] and by taking into account our detection geometry and energy discrimination. This contribution was found to be (20 ± 4)% of the pair yield in the spectrum.

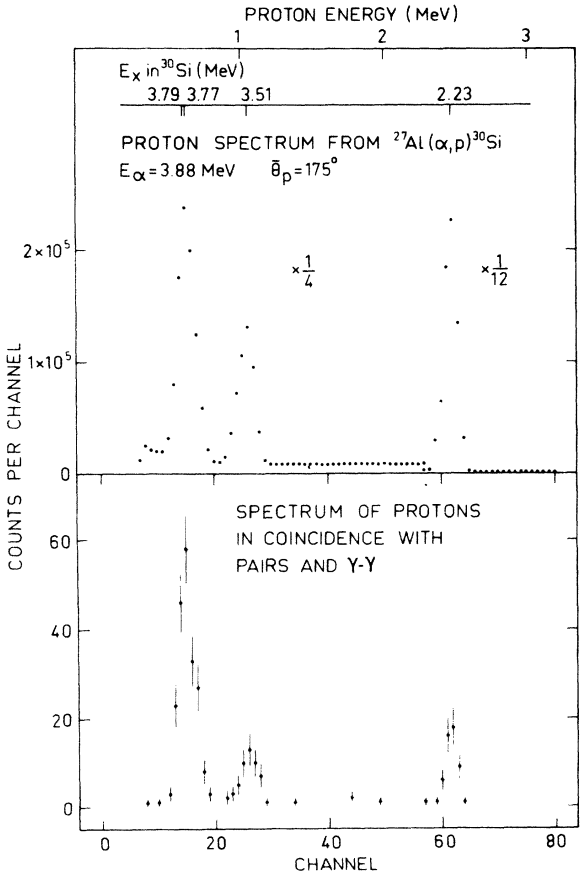

FIG. 8. (a) 1/4 (and 1/12 for one peak) sampled direct proton spectrum from ^{27}Al(α, p)^{30}Si taken simultaneously with the nonrepresented proton energy vs pair energy spectrum. (b) Projection on the proton energy axis of the two-dimensional spectrum. The π decay relevant to the 3.79 MeV state is around channel 15 in the figure.

Our final result for the pair branching ratio of the ^{30}Si(3.79 MeV, 0^+) state is $\Gamma_\pi/\Gamma = (2.6 \pm 0.6) \times 10^{-3}$. A recent measurement of this ratio at Brookhaven[43] gives $(2.7 \pm 0.4) \times 10^{-3}$. To our knowledge three lifetime measurements exist for the first excited 0^+ state in ^{30}Si. They are $\tau_m = (24.2 \pm 2.0)$ psec,[44] (6.8 ± 2.0) psec,[45] and (15.6 ± 1.2) psec.[37] By taking the last and most recent value for τ_m the above branching ratio yields $\tau_\pi = (6.0 \pm 1.5)$ nsec for the partial mean lifetime of the ground state $E0$ decay. The value of the $E0$ matrix element is $\langle M \rangle_\pi = (1.4 \pm 0.2)$ fm^2.

III. CONCLUSION

Table I shows the properties of the 0^+ states studied in this work compared to the properties of the first excited 0^+ state at $E_x = 3.35$ MeV in the $4n+4$ nucleus ^{36}S. As can be seen from the table, the monopole strength in single particle units of the first excited 0^+ state in ^{30}Si and ^{36}S are quite small. A shell model argument[18] can explain the fact that the monopole strength in ^{36}S is small. Such argumentation should hold roughly

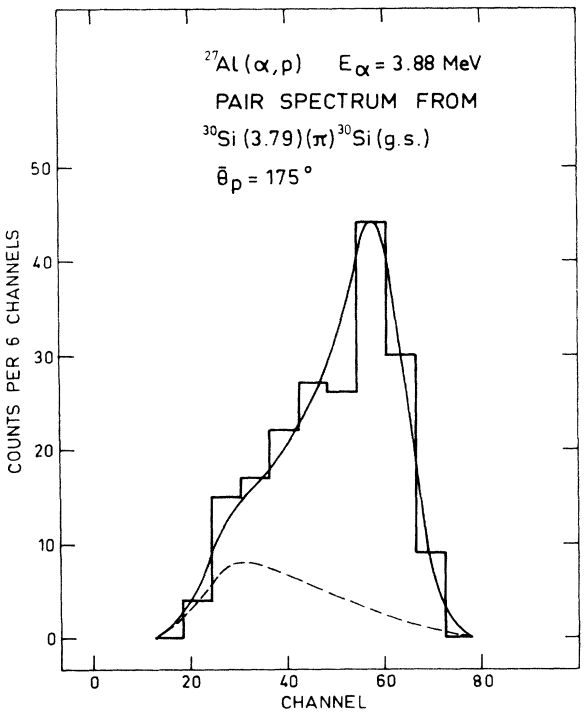

FIG. 9. Pair spectrum obtained from the projection of the events between channels 12–20 of Fig. 8(b) onto the pair energy axis of the relevant proton energy vs pair energy spectrum (not represented). The dashed line is the calculated contribution of the γ interactions in the telescopes due to γ-ray decays of the unresolved 3.77 and 3.79 MeV states. The solid line is taken from the spectrum of Fig. 3.

TABLE I. Properties of the first excited $J^\pi = 0^+$ states in three nuclei of the s-d shell.

Nucleus	E_x (MeV)	τ_m (psec)	Ref.	Γ_π/Γ	Reference	$\langle M \rangle_\pi$ (fm^2)	$E0$ strength (s.p. units)
^{26}Mg	3.58	9.6 ± 1.2	38	$(5.1 \pm 0.7) \times 10^{-3}$	This work	3.0 ± 0.25[a]	$(2.9 \pm 0.5) \times 10^{-1}$
		9.5 ± 0.7	37				
^{30}Si	3.79	24.2 ± 2.0	44				
		6.8 ± 2.0	45				
		15.6 ± 1.2	37	$(2.6 \pm 0.6) \times 10^{-3}$	This work	1.4 ± 0.2[b]	$(5.3 \pm 1.3) \times 10^{-2}$
^{36}S	3.35	12 700 ± 300	46	1	24, 26	1.38 ± 0.03	$(3.8 \pm 0.1) \times 10^{-2}$

[a] Value obtained by taking for τ_m the mean weighted value of lifetimes given in Refs. 37 and 38.
[b] Value obtained for $\tau_m = (15.6 \pm 1.2)$ psec (Ref. 37).

for both the ^{30}Si and ^{26}Mg cases. However the measured $E0$ strength in ^{26}Mg is about six times bigger than those in ^{30}Si and ^{36}S. This implies that a more sophisticated explanation is needed to understand the behavior of monopole transitions in the s-d shell. As suggested by the strong $E0$ decay in ^{18}O and ^{42}Ca, the breakup of the core might play an important role in this kind of transition. It is our feeling that more experimental data on such transitions would be a very useful tool in a systematic theoretical investigation of the structure of the 0^+ states involved. Moreoever, one expects, from the form itself of the monopole operator, to get some insight on whether or not the mean configuration radii changes for the subshells of the closed shell.

We would like to thank Dr. A. Pape for critical reading of the manuscript.

[1]S. J. McCaslin, F. M. Mann, and R. W. Kavanagh, Phys. Rev. C 7, 489 (1973).
[2]M. Stroetzel, Z. Phys. 214, 357 (1968).
[3]J. H. Fregeau, Phys. Rev. 104, 225 (1956).
[4]H. L. Crannell and T. A. Griffy, Phys. Rev. 136, B1580 (1964).
[5]F. Gudden and P. Strehl, Z. Phys. 185, 111 (1965).
[6]H. L. Crannell, T. A. Griffy, L. R. Suelzle, and M. R. Yearian, Nucl. Phys. A90, 152 (1967).
[7]R. F. Frosch, R. E. Rand, H. L. Crannell, J. S. McCarthy, L. R. Suelzle, and M. R. Yearian, Nucl. Phys. A110, 657 (1968).
[8]S. Devons, G. Goldring, and J. R. Lindsey, Proc. Phys. Soc. Lond. A67, 134 (1954).
[9]R. M. Kloepper, R. B. Day, and D. A. Lind, Phys. Rev. 114, 240 (1959).
[10]S. Gorodetzky, N. Schulz, J. Chevallier, and A. C. Knipper, J. Phys. (Paris) 27, 521 (1966).
[11]M. Goldhaber and R. D. Hill, Rev. Mod. Phys. 24, 179 (1952).
[12]M. Deutsch, Nucl. Phys. 3, 83 (1957).
[13]D. E. Alburger, Phys. Rev. 109, 1222 (1958).
[14]E. K. Warburton and D. E. Alburger, in *Nuclear Spin-Parity Assignments: Proceedings of the Conference on Bases for Nuclear Spin-Parity Assignements, Gatlinburg, Tennessee, 1965*, edited by N. B. Gove and R. L. Robinson (Academic, New York, 1966), p. 114.
[15]D. E. Alburger and E. K. Warburton, Phys. Rev. 185, 1242 (1969).
[16]D. E. Alburger, Phys. Rev. 118, 235 (1960).
[17]D. E. Alburger, A. Gallmann, J. B. Nelson, J. T. Sample, and E. K. Warburton, Phys. Rev. 148, 1050 (1966).
[18]E. K. Warburton and D. E. Alburger, Phys. Lett. 36B, 38 (1971).
[19]E. K. Warburton and D. E. Alburger, Phys. Rev. C 6, 1224 (1972).
[20]S. Gorodetzky, R. E. Pixley, A. Gallmann, G. Frick, J. P. Coffin, and G. Sibille, J. Phys. (Paris) 24, 892 (1963).
[21]N. Benczer-Koller, G. G. Seaman, M. C. Bertini, J. W. Tape, and J. R. McDonald, Phys. Rev. C 2, 1037 (1970).
[22]B. N. Belyaev, S. S. Vasilenko, D. M. Kaminker, Izv. Akad. Nauk. SSSR Ser. Fiz. 35, 806 (1971) [transl.: Bull. Acad. Sci. USSR, Phys. Ser. 35, 742 (1971)].
[23]N. Benczer-Koller, M. Nessin, and T. H. Kruse, Phys. Rev. 123, 262 (1961).
[24]E. A. Samworth and J. W. Olness, Phys. Rev. C 5, 1238 (1972).
[25]D. H. Wilkinson, Nucl. Instrum. Methods 82, 122 (1970).
[26]M. Nessin, T. H. Kruse, and K. E. Eklund, Phys. Rev. 125, 639 (1962).
[27]S. Devons, H. G. Hereward, and G. R. Lindsey, Nature (Lond.) 164, 586 (1949).
[28]S. Devons and G. R. Lindsey, Nature (Lond.) 164, 539 (1949).
[29]S. Devons and G. Goldring, Proc. Phys. Soc. Lond. A67, 413 (1954).
[30]S. Gorodetzky, P. Chevallier, R. Armbruster, A. Gallmann, and G. Sutter, Nucl. Phys. 7, 672 (1958).
[31]S. Gorodetzky, F. Scheibling, P. Chevallier, P. Mennrath, and G. Sutter, Phys. Lett. 1, 25 (1962).
[32]S. Gorodetzky, P. Chevallier, R. Armbruster, G. Sutter, and A. Gallmann, Nucl. Phys. 8, 412 (1958).
[33]S. Gorodetzky, P. Chevallier, R. Armbruster, and

G. Sutter, Nucl. Phys. 12, 12 (1959).
[34]A. Muser, J. Zen, J. D. Michaud, and F. Scheibling, Nucl. Instrum. Methods 63, 273 (1968).
[35]J. Marshall and A. G. Ward, Can. J. Res. A15, 39 (1937).
[36]P. M. Endt and C. Van der Leun, Nucl. Phys. A214, 1 (1973).
[37]F. Beck, P. Engelstein, and J. P. Vivien, Nucl. Phys. A228, 393 (1974).
[38]Z. Berant, C. Broude, G. Engler, and M. J. Renan, Nucl. Phys. A218, 324 (1974).
[39]D. H. Wilkinson, Nucl. Phys. A133, 1 (1969).
[40]J. F. Sharpey-Schaefer, P. R. Alderson, D. C. Bailey, J. L. Durell, M. W. Green, and A. N. James, Nucl. Phys. A167, 602 (1971).
[41]F. Ajzenberg-Selove, Nucl. Phys. A190, 1 (1972).
[42]M. E. Rose, Phys. Rev. 76, 678 (1949).
[43]E. K. Warburton and D. E. Alburger, Phys. Rev. C 10, 1570 (1974).
[44]F. Haas, B. Heusch, G. Frick, A. Gallmann, and D. E. Alburger, Nucl. Phys. A156, 385 (1970).
[45]N. Anyas-Weiss, R. Griffiths, N. A. Jelly, W. Randolph, J. Szücks, and T. K. Alexander, Nucl. Phys. A201, 513 (1973).
[46]J. W. Olness, W. R. Harris, A. Gallmann, F. Jundt, D. E. Alburger, and D. H. Wilkinson, Phys. Rev. C 3, 2323 (1971).